I-1. PROJECT RESEARCHES

Project 2

PR2 Development on Neutron Imaging Application

Y. Saito

Institute for Integrated Radiation and Nuclear Science, Kyoto University

1. Objectives and Allotted Research Subjects

Neutron imaging provides valuable information which cannot be obtained from an optical or X-ray imaging. The purpose of this project is to develop the imaging method itself and also the experimental environment for expanding the application area of the neutron imaging. The allotted research subjects are as follows:

ARS-1 Measurements of Multiphase Dynamics by Neutron Radiography (Y. Saito *et al.*)
ARS-2 Visualization and Measurement of Flow Behavior in Industrial Equipment (H. Asano *et al.*)
ARS-3 Visualization and Measurement of Adsorption/Desorption Process of Ethanol in Activated Carbon Adsorber for Adsorption Heat Pump (N. Asano *et al.*)
ARS-4 Visualization of heavy oil in packed bed reactor by neutron radiography (T. Tsukada *et al.*)
ARS-5 Characteristics of the Void Fraction under Transient Condition (H. Umekawa *et al.*)
ARS-6 Estimation of the Frosting and Defrosting Phenomena by Using Neutron Radiography (R. Matsumoto *et al.*)
ARS-7 Neutron imaging and optics development using simulation of VCAD Systems (Y. Yamagata *et al.*)
ARS-8 Water and Salt Distribution in a Rice Hull Medium under Sodium Chloride Solution Culture (U. Matsushima *et al.*)
ARS-9 Measurement of Water Content in Hardened Cement Paste by Neutron Imaging (T. Numao *et al.*)
ARS-10 In-situ Neutron Radiography Investigation on the Hydraulic Behavior of High Strength Cement Paste under High Temperature (M. Kanematsu *et al.*)
ARS-11 Evaluation of coolant distribution in a flat heat-pipe type heat spreader (K. Mizuta *et al.*)
ARS-12 Visualization of Organic Materials for Development of Industrial Applications (A. Uritani *et al.*)
ARS-13 Visualization of Coolant Flow in a Micro-Structured Wick (Y. Tsuji *et al.*)

2. Main results and the contents of this report

To develop neutron imaging, our imaging system was developed so that high-speed imaging could be performed at thermal neutron flux of 10^7 n/cm^{2}s. Such improved system was shared with all of the project members and valuable results were obtained as follows:

ARS-1 improved the above-mentioned high-speed imaging system at the B4 port. The spatial and temporal resolution of the system was tested. Then, the present system was applied to investigate the effect of motion blur in the observation of rapidly moving object and to visualize air-water two-phase flow structure.

ARS-2 applied to neutron imaging to simultaneous measurements of water distribution in Polymer Electrolyte Fuel Cell (PEFC). From the measurement results, the existing correlations for the protonic conductivity of PEFC overestimates the measured values. This results indicate that change in the protonic conductivity with respect to the water content becomes small in low range of water content.

ARS-3 applied neutron imaging to measurements of distribution of adsorbed refrigerant in adsorbent particle layer. The dynamic behavior of the refrigerant during the adsorption was clearly visualized.

ARS-4 applied neutron imaging to the flow visualization of heavy oil in packed bed reactor. Heavy oil were supplied to the packed bed reactor filled with supercritical water. From the experimental results, a flow channeling was observed depending on the experimental conditions.

ARS-5 applied the neutron imaging to boiling two-phase flow at a high temperature conditions. High-speed quenching phenomena was successfully visualized by using our improved imaging system. In addition to such boiling experiments, quantitative method for void fraction was examined.

ARS-6 applied neutron imaging to frosting behavior in cooling heat exchange system. 3-D frost density was clearly visualized by the neutron CT imaging system at the B4 port.

ARS-8 applied neutron imaging to observation of water movement in reciprocal grafts of tomato and eggplant by analyzing movement of D_2O as tracer.

ARS-12 performed quantification of neutron imaging by using two-different neutron source (KUR-E2 and NUANS). Carbon fiber reinforced plastic and its peeling from aluminum alloy was visualized. The spatial resolution of neutron imaging at the two neutron imaging facilities was compared each other.

ARS-13 wanted to develop new measurement technique of the superfluid. However, the experiments could not be performed due to malfunction of laser system.

PR2-1 Measurements of multiphase flow dynamics using neutron radiography

Y. Saito and D. Ito

Institute for Integrated Radiation and Nuclear Science, Kyoto University

INTRODUCTION: Neutron radiography (NRG) is a powerful tool for fluid flow visualization as well as two-phase flow research. Gas-liquid two-phase flows in a metallic pipe have been visualized clearly by using NRG. However, it would be still difficult to obtain dynamic information on such flows by NRG, because of insufficient neutron flux from neutron sources or poor efficiency of imaging devices. In this work, our imaging system was improved for high frame rate NRG. Then, the improved system was applied to investigate the effect of motion blur in the observation of rapidly moving object and to visualize air-water two-phase flow structure.

HIGH-SPEED NEUTRON IMAGING: A high frame rate NRG system was constructed at the B-4 supermirror neutron guide facility [1] of the Institute for Integrated Radiation and Nuclear Science, Kyoto University. In the B-4 port, the neutron flux is 8.5×10^7 n/cm^{2}s at 5MW reactor operation mode, and the beam width and height at the beam exit are 10 mm and 75 mm, respectively. The imaging system for high frame rate NRG consists of a neutron converter, a dark box with a single mirror, an ultrasensitive lens, an optical image intensifier and a high-speed camera. In this system, a high sensitivity high-speed camera (AX-50, Photron) was applied to enhance the temporal resolution. The frame rate of 10,000 fps was achieved using this system at the B-4 port [2]. The spatial resolution and frame rate can be adjusted by selecting the optics.

EVALUATION OF MOTION BLUR: The motion blur cannot be neglected in the imaging of high-speed moving object. A Gd indicator illustrated in Fig.1(left) was rotated using a rotating disc system and the neutron transmission image of the rotating indicator was obtained. A typical image of the static indicator is shown in Fig.1(right). The shape of the Gd indicator could be clearly observed by neutron radiography. The transmission images of the rotating indicator with different velocity are shown in Fig.2. The indicator moved downward and the transmission images were obtained at the frame rate of 10,000 fps. As the rotating velocity increases, the image degradation becomes significant. The effect of this blur should be clarified for accurate measurements by high frame rate NRG.

TWO-PHASE FLOW VISUALIZATION: Air-water two-phase flow was visualized by the present high frame rate NRG system. The test section is a vertical circular pipe which is made from aluminum. The inner diameter is 10 mm and the wall thickness of the test pipe is 1 mm. The water was circulated by a pump and the compressed air was injected from the upstream of the test section. The flow rates of water and air were monitored by flow meters. The typical void fraction distribution estimated from the neutron transmission image is shown in Fig.3. The superficial liquid and gas velocity are 0.72 m/s and 15.3 m/s, respectively, and the flow pattern in the test section was annular flow. The gas phase passes through the center of the cross-section and the liquid film flows along the wall. Fast fluctuation behavior of such liquid film was observed by the high frame rate NRG.

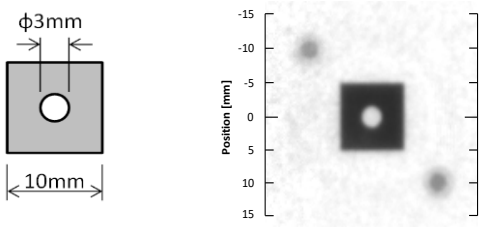

Fig. 1 Detail (left) and neutron transmission image (right) of the Gd indicator.

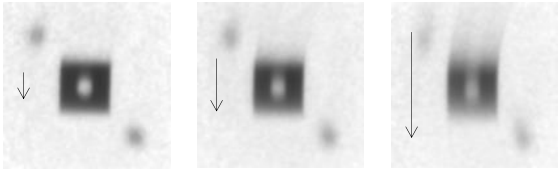

Fig. 2 Neutron transmission images of rotating indicator.

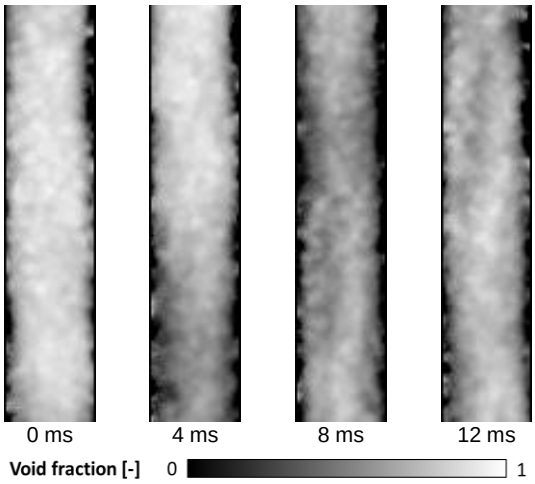

Fig. 3 Void fraction distributions in annular flow (J_L=0.72m/s, J_G=15.3m/s).

REFERENCES:

[1] Y. Saito, *et al*., Nucl. Instr. Meth. Phys. Res., A, **651** (2011) 36-41.

[2] D. Ito, Kei Ito and Y. Saito, WCNR-11, Sydney, Australia (2018).

Simultaneous Measurements of Water Distribution and Electrochemical Characteristics in Polymer Electrolyte Fuel Cell

H. Murakawa, S. Sakihara, K. Sugimoto, H. Asano, D. Ito[1] and Y. Saito[1]

Graduate School of Engineering, Kobe University
[1]Institute for Integrated Radiation and Nuclear Science, Kyoto University

INTRODUCTION: Water management in polymer electrolyte fuel cells (PEFCs) is a key topic for the PEFC operation. If condensed water exists in the gas diffusion layer (GDL) and the gas channel, it may depress the gas diffusion as flooding. In order to clarify the effect of water content in the proton exchange membrane (PEM) and the (GDL) on the electric resistances, simultaneous measurements of water distribution and the electrical impedance were carried out by using the neutron radiography and electrochemical impedance spectroscopy (EIS). Change of water accumulation in the PEM and the GDL were compared with the PEM and the reaction resistances.

EXPERIMENTS: A small size PEFC having nine-parallel gas-channels with cross-sectional area of 1 × 1 mm^2 was used for measuring two-dimensional water distribution and the electrochemical characteristics. Nafion® NR-212 was used as the PEM with a thickness of approximately 90 μm having catalyst layers on both the anode and cathode sides. The GDL was carbon paper (Toray Ind.) with thickness of 190 μm at the cathode side and 280 μm at the anode side. The porosity of the GDL was approximately 78%. Two-dimensional water distributions were obtained every 60 sec during the PEFC operation. The EIS measurements were simultaneously carried out with the neutron radiography for evaluating the PEM resistance R_{PEM} [Ω] and the reaction resistance R_{CT} [Ω]. The EIS was carried out with a frequency range of 0.5 to 30 kHz.

RESULTS: Two-dimensional water distributions at current density i =158 mA/cm^2 are shown in Fig. 1. Liquid water accumulation during the PEFC operation can be confirmed as indicated by the gray-scale. Amounts of water accumulation in the GDL under the lands and channels are different and a large amount of water existed under lands at the earlier results. It indicated that water accumulation is started under the lands. Then, liquid water reaches channel and are particularly concentrated on the land corners.

Fig. 2 shows time series of the cell voltage, R_{PEM} and R_{CT}. The cell voltage rapidly recovered just after the PEFC operation and was almost constant. R_{CT} slightly increased although R_{PEM} slightly decreased with the operation time. Water contents in the PEM, λ, were evaluated from the water distributions. Change of λ and σ based on the initial condition, Δλ and Δσ, are shown in Fig. 3. It can be confirmed that Δσ almost linearly increases with Δλ. This tendency is the same with a proposed correlation by Springer et al. [1]. However, effect of water contents on the protonic conductivity was much less that the literature. This results show that change in the protonic conductivity with respect to the water content becomes small in low range of water content.

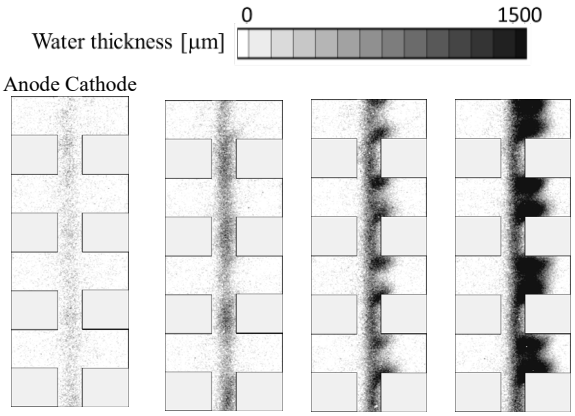

Fig. 1. Two-dimensional water distributions at i =158 mA/cm^2.

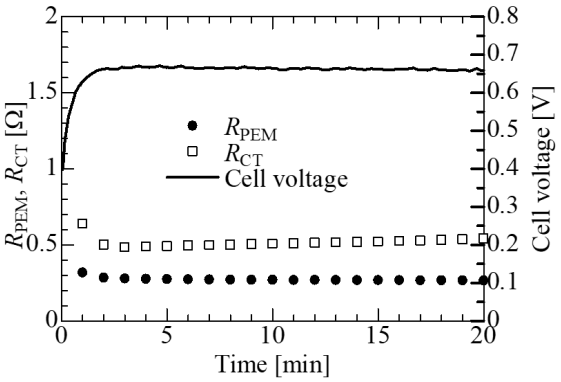

Fig. 2 Relation between the cell voltage and the resistance at i =158 mA/cm^2.

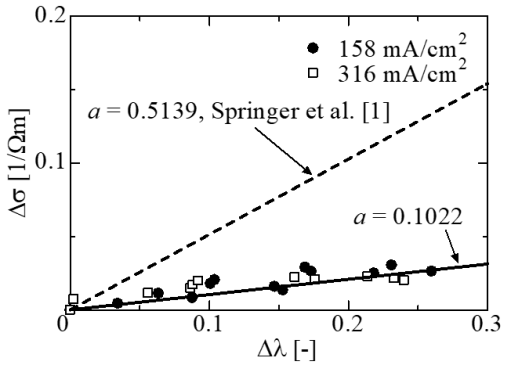

Fig. 3. Relation between water content in MEA and the protonic conductivity.

REFERENCE:

[1] T.E. Springer, T.A. Zawodzinski and S. Gottesfeld, J. Electrochem. Soc., **138** (1991) 2334-2342.

PR2-3

Visualization and Measurement of Distribution of Adsorbed Refrigerant in Adsorbent Particle Layer under Transient Conditions

H. Asano, G. Ren, H. Murakawa, K. Sugimoto,
D. Ito[1] and Y. Saito[1]

Graduate School of Engineering, Kobe University

[1]Institute for Integrated Radiation and Nuclear Science, Kyoto University

INTRODUCTION: Adsorption refrigerator driven by heat at relatively low temperature is one of the efficient tools for waste heat recovery. Refrigerant vapor from an evaporator at low pressure is adsorbed in an adsorbent particle layer in an adsorber. In order to keep the evaporation pressure, the adsorber must be changed to a dry adsorber in a batch operation. Wet adsorber is regenerated by heating. Therefore, the coefficient of performance is low due to its batch operation and the heat capacity of the adsorber. On the other hand, although adsorbed amount increased with decreasing the adsorbent temperature for a refrigerant pressure, the adsorbent is heated by the adsorption heat in the adsorption process. So, quick rejection of the adsorption heat from the adsorbent layer is required in the adsorption process. Metallic fins are often used for higher thermal diffusion. In is required for the optimal design of the fin configuration to clarify adsorption/desorption phenomena in transient changes. Adsorbed refrigerant distribution in an adsorbend particle layer in a cylindrical cell was visualized by neutron radiography.

EXPERIMENTS: Activated carbon and ethanol were used as the adsorbent and refrigerant, respectively. Mean particle diameter of the activated carbon was 86 μm. Activated carbon was installed in a cylindrical cell with thin stainless steel wall and the inner diameter of 21 mm. The depth of the adsorbent layer was 35 mm. The installed amount of dry activated carbon was 3 g. The layer was covered by two aluminum porous plates with the thickness of 10 mm to prevent scatter by vapor flow. The bottom of the cell was brazed on a brass plate whose temperature was maintained by cooling water. The cell was connected to a liquid ethanol reservoir immersed in a temperature controlled water.
The mass attenuation coefficient of liquid ethanol was 3.86 cm^2/g [1]. Radiographs on a scintillation converter were recorded by a cooled CCD camera with the exposure time of 30 seconds and the pixel size of 42.8 μm/pixel. The temperatures of the bottom plate and ethanol reservoir were maintained at 30 °C and 10 °C during the adsorption process, respectively.

RESULTS: Original radiographs under the condition of dry before adsorption and with adsorbed ethanol are shown in Fig. 1 (a) and (b), respectively. It was clearly show that the region of adsorbent layer became darker due to ethanol adsorption. Adsorbed amount was larger closer to the surface. Heat radiation through the side wall to the ambient air might be enough for the heat rejection of the adsorption heat. Attenuation due to ethanol was calculated for each pixel and summed values in the sliced layer with 3 mm height (70 pixels) were evaluated. Temporal change of the summed values are plotted against the elapsed time from the adsorption start in Fig. 2. The value at 31.6 mm was lower because the region included the surface and the adsorbent amount was smaller. It was clearly shown that refrigerant adsorption progressed from the surface to the depth. Figure 3 shows the horizontal distribution at each sliced layer at 2670 seconds from the start. Smooth bold lines show the proportional profile of the chord length of cell along the beam direction. At 28.6 and 25.7 mm, the adsorption ratio might be higher near the wall. On the other hand, at 16.9 mm, the adsorption ratio seemed to be homogeneous because the attenuation distribution agreed well with the cell size.

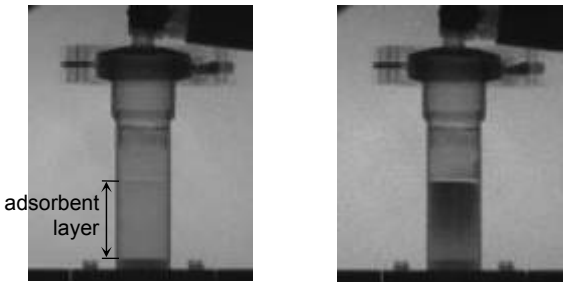

(a) Before adsorption (b) With adsorption

Fig. 1 Obtained neutron radiographs at E2 port of KUR.

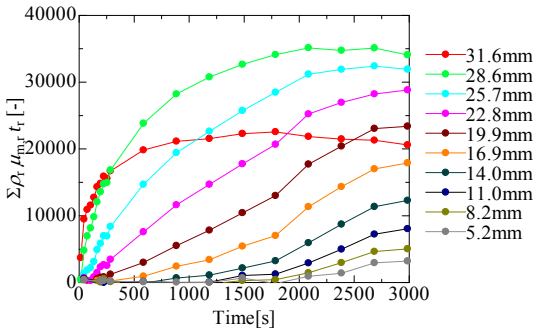

Fig. 2 Change of adsorbed amount at different height.

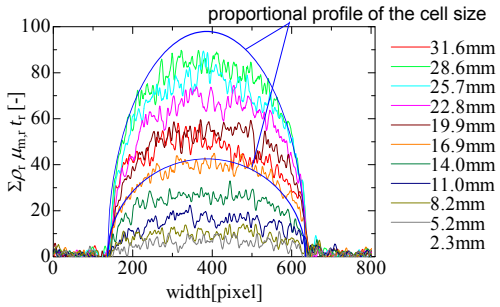

Fig. 3 Horizontal distribution of adsorbed amount.

REFERENCE:

[1] H. Asano, K. Murata, N. Takenaka and Y. Saito, Physics Procedia, **69** (2015) 503-508.

PR2-4 Flow visualization of heavy oil in supercritical water using neutron radiography

T. Tsukada, M. Kubo, E. Shoji, T. Kikuchi, N. Ito, S. Takami[1], K. Sugimoto[2], D. Ito[3] and Y. Saito[3]

Dept. of Chemical Engineering, Tohoku University

[1] Dept. of Materials Science and Engineering, Nagoya University

[2] Dept. of Mechanical Engineering, Kobe University

[3] Institute for Integrated Radiation and Nuclear Science, Kyoto University

INTRODUCTION: With an increase in the demand for petrochemical feedstock and middle distillate, utilization of heavy oil such as atmospheric or vacuum residue is also necessary. Since the heavy oil has high viscosity and its quality is low, desulfurization and upgrading processes are required to use the heavy oil effectively. In such a situation, upgrading process using supercritical water has been proposed and studied recently.

Understanding of flow behavior of heavy oil in reactors filled with supercritical water is important to improve the performance of upgrading process. However, the phenomena are complicated to simulate numerically. Since, in experiment, the reactor is made of metal for operation at high pressure and high temperature, the visualization using visible light is not available. Thus, the numerical simulation and experimental flow visualization of heavy oil flow in supercritical water have not been conducted. In our previous study [1], we have visualized the heavy oil flow in a trickle bed reactor under N_2 atmosphere using neutron radiography, and indicated the potential of neutron radiography to investigate the flow behavior of heavy oil. As a next step, the objective of this study is to visualize the heavy oil flow in supercritical water.

EXPERIMENTS: In neutron radiography for the flow visualization of heavy oil in supercritical water, the Kyoto University Research Reactor (KUR) was utilized as neutron source. A series of neutron radiography experiments was conducted with a thermal neutron flux of 5×10^7 n/cm^2·s.

Fig. 1 shows the schematic diagram of the apparatus used in the experiment. The reactor consists of a 1/2-inch stainless steel tube filled with Al_2O_3 particles having the diameter of 3 mm. The heavy oil was supplied to a reactor from above with the flow rates of 2.5 or 5.0 mL/min. Atmospheric residue (AR) was used as the heavy oil sample. On the other hand, the water was supplied counter-currently with the flow rates ranged from 0.05 to 7.5 mL/min. The reactor was heated to temperatures of 400°C and was operated at 25 MPa.

An image intensifier and a camera at the framerate of 30 fps were used to obtain radiography images of the unsteady flow behavior. An image processing to reduce noises and to calculate neutron attenuation was performed for the obtained radiography images.

RESULTS: The flow behavior of heavy oil in the reactor varied depending on the experimental conditions were visualized using neutron radiography. Fig. 2 shows the time variation of flow behavior of heavy oil in supercritical water at the flow rates of heavy oil and water were 2.5 mL/min and 1.0 mL/min, respectively. The heavy oil spread radially to the wall of the tube. This is because heavy oil diffused in supercritical water. In addition, the heavy oil spread above the nozzle because the lighter components contained in the heavy oil were carried by the supercritical water flow.

CONCLUSION: This study indicated that neutron radiography is a useful technique to visualize the flow behavior of heavy oil in metallic reactor filled with supercritical water at high pressure and high temperature conditions. The results showed that the flow behavior of heavy oil depends on the flow rates of heavy oil and supercritical water.

ACKNOWLEDGEMENT: This research was supported by Kurita Water and Environment Foundation.

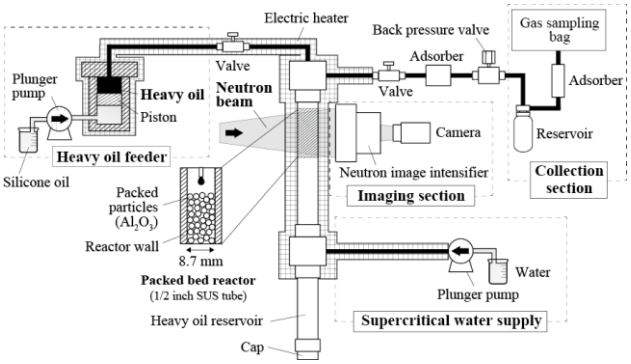

Fig. 1: Schematic diagram of experimental apparatus

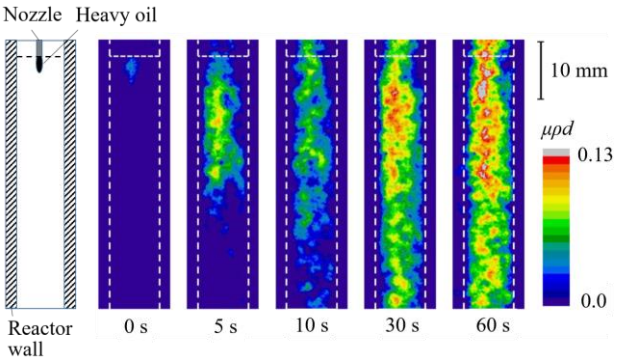

Fig. 2: Flow behavior of heavy oil in supercritical water when the flow rates of heavy oil and water were 2.5 mL/min and 1.0 mL/min, respectively. μ, ρ, and d are mass attenuation coefficient of thermal neutrons [m^2/kg], density of heavy oil [kg/m^3], and thickness along the neutron beam direction

REFERENCES:

[1] E. Shoji *et al.*, Chem. Eng. Sci., **196** (2019) 425-432.

Quantitative Dynamic Measurement of Void Fraction

H. Umekawa, T. Ami, K. Saito, Y. Kawazoe, K. Obata, K. Shibata, H. Sakai, Y. Saito[1] and D. Ito[1]
Dept. Mechanical Engineering, Kansai University.
[1]*Institute for Integrated Radiation and Nuclear Science, Kyoto University.*

INTRODUCTION: In this series of experiments, Void fraction of forced convective boiling is quantitatively visualizing under three kind of conditions, i.e. Micro-channel heat exchanger, Quenching process and Sub-cooled boiling. In each experiment, several technical trials as the neutron radiography technique are included, and one of them is quantitative measurement of dynamic image. In this report, the estimation results of the ability of the dynamic image processing is briefly explained.

EXPERIMENTS: In the quenching experiment, sub-cooled liquid was injected into the superheated test section which was heated until 800 deg.C. After the injection, quenching was propagated, and Inverted annular flow might be constructed in the test section. In this kind of experiment, to estimate the Inverted annular flow, "hot-patch" to prevent the propagation of quenching has been normally equipped so far, but the detail information at the quenching point could not be acquired by this method. In this mean, the dynamic quantitative measurement has been strongly required.

Figure 1 is the visualization result by using the high speed camera (Photron AX-50) with 10,000 frames/sec. Although the movement of liquid slug is clearly observed, it's not enough for the quantitative measurement.

To estimate the required neutron number for quantitative measurement, the neutron flux at the arbitrary location from beam exit has been simply estimated by using the geometric relationship of beam expansion as shown in Fig.2.

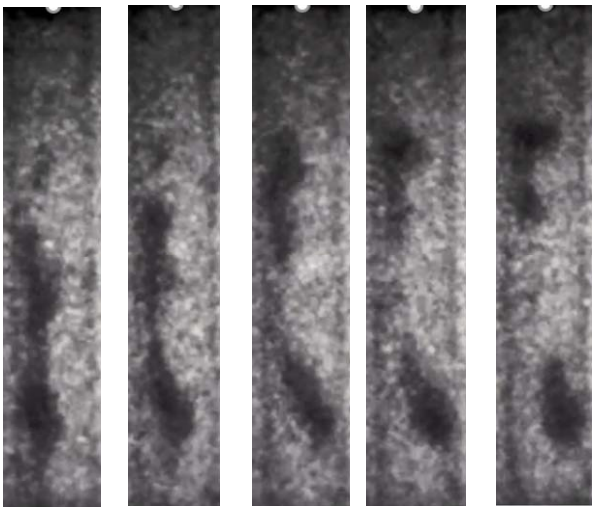

Fig. 1. Example of visualization image at 10,000 frame/s.

On the basis of these neutron flux, the relationship between the frame rate and pixel size is explained at Fig.3. For the purpose of flow observation, approximately 5neutrons/pixel is enough, and this condition corresponds to the condition of Fig.1. The requirement of the quantitative measurement is estimated by using visualization image of 500frames/sec with 0.5ms exposure period, and evaluated by using the standard deviation. As the results, 0.5ms exposure period is not enough and 2.5ms is minimum exposure period for quantitative measurement, and over 10ms is more suitable exposure period. The neutron number under these exposure period corresponds to a.20n/pixel, a.100n/pixel and a.300n/pixel, respectively. This number would be used as the standard value to consider the frame rate of dynamic quantitative measurement.

Author wish to express sincere thanks to Messrs H. Fuiwara and T. Kageyama for their support in the experiment.

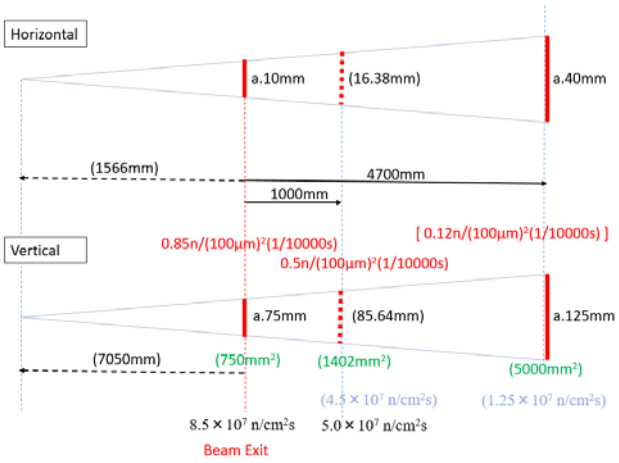

Fig. 2 Rough estimation of visible area and neutron flux.

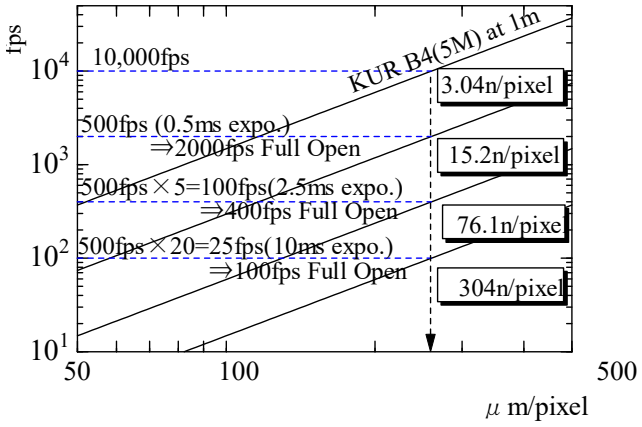

Fig. 3 Requirement of neutron number for qualitative measurement.

PR2-6 Three Dimensional Frost Formation on the Heat Exchanger Measured by Neutron CT

R. Matsumoto, Y. Nagasawa[1], T. Shiokawa[1], Y. Nishiura[1], D. Ito[2] and Y. Saito[2]

Faculty of Engineering Science, Kansai University
[1]Graduate School of Science and Engineering, Kansai University
[2]Institute for Integrated Radiation and Nuclear Science, Kyoto University

INTRODUCTION: Heat exchangers which are operated at 0 deg.C below are subjected to the frost deposition and its growth. The frost layer is a porous structure of ice crystals and air pores. The frost layer has low conductivity, thus, the frost formation on heat exchanger causes serious problem to the heat transfer performance by thermal resistance between the cold surface and the humid ambient air. Matsumoto et al. [1] reported the two dimensional distribution of the frost deposition rate on the plate fin-tube heat exchanger by using neutron radiography. Neutrons are strongly attenuated by the water molecules in the frost layer, but not by the aluminum heat exchanger. The frost formation can be quantitatively estimated based on the neutron beam attenuation. By applying the computed tomography technique, three dimensional frost formation can be visualized. In this study, the three dimensional distribution of the frost deposition and the frost density profiles on the plate fin-tube heat exchanger are quantitatively estimated by using the neutron computed tomography at KUR B-4 radiation port.

EXPERIMENTS: Fig.1 shows the schematic view of the experimental apparatus. Cooled humid air adjusted to the flow rate 70 L/min was supplied to the test section. The test section consisted of Styrofoam block duct with a cross section of 68 mm x 150 mm and the aluminum plate fin-tube heat exchanger. The heat exchanger consisted by 6 fins with 60 mm in height, 28 mm in width, 0.25 mm in thickness, and together with two tubes of an outer 8.5 mm. Fig.2 shows the aluminum heat exchanger used in this experiment. Fin pitch was 5 mm. The heat exchanger was cooled by -22 ºC fluorinert. The frosting duration was 60 min. CCD camera (Princeton Inst., 16-bit, 1024 × 1024 pixels) set in the inside a light-tight camera box. Two mirrors reflect the visible ray image from the converter with the 6LiFZnS scintillator screen mounted onto the front end of the camera box. 600 neutron radiography (NRG) images were taken by the CCD camera with an exposure time of 5 sec by rotating the heat exchanger through 180 degrees.

RESULTS: Fig.3 shows the three dimensional frost formation on the heat exchanger with the horizontal cross section at z=17.5, 30, 42.5 and 60mm. The tomographic image shows the linear attenuation coefficient μ. The frost density ρ can be calculated from $\rho = \mu / \mu_{m,ice,}$ in which $\mu_{m,ice}$ is the mass attenuation coefficient of ice. At the front fin edge, high frost deposition are observed. Inside of the heat exchanger, the frost layer covered whole of the fin surface, however, the frost layer is thin in the wide area of the wake region of the tubes. The three dimensional frost density profile can be estimated by using 3D neutron computed tomography.

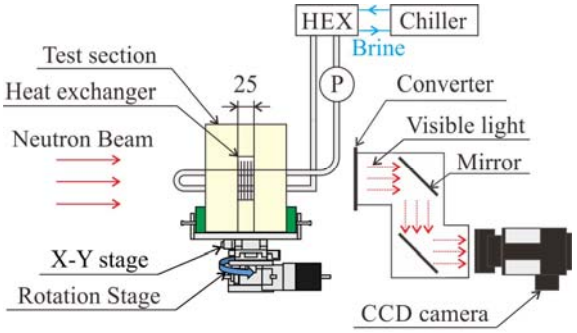

Fig.1 Schematic view of the experimental apparatus.

Fig. 2 Plate-fin tube heat exchanger.

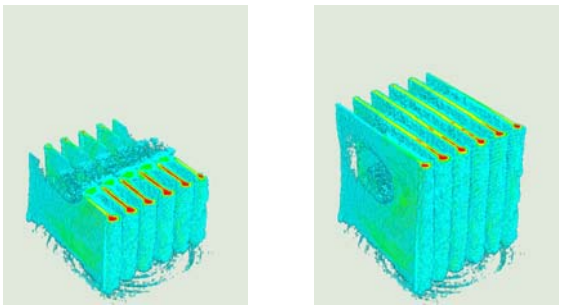

(a) z = 17.5mm (b) z = 30mm

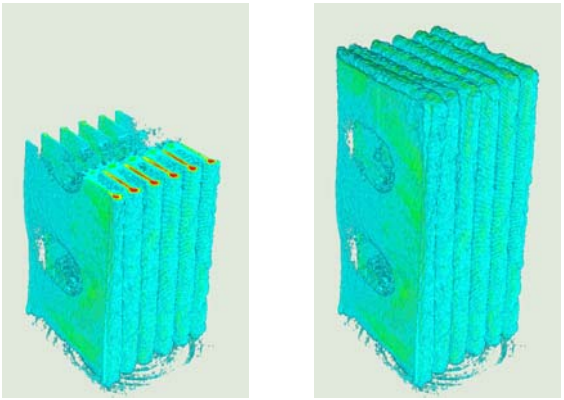

(a) z = 42.5mm (b) z = 60mm

Fig.3 Three dimensional frost density distributions.

REFERENCE:
[1] R. Matsumoto, et al., Proceedings of the International Heat Transfer Conference IHTC-15, IHTC15-9144, Kyoto, pp. 3603-3615.

PR2-7 Analysis of production technology of optics components using neutron radiography

Y. Yamagata[1], Y. Saito[3], T. Hosobata[1], S. Takeda[1], S. Morita[1,2], M. Hino[3] and D. Ito[3]

[1]*RIKEN Center for Advanced Photonics, RIKEN*
[2]*Tokyo Denki University*
[3]*Institute for Integrated Radiation and Nuclear Science, Kyoto University*

INTRODUCTION:

Precision optics are important key components used in imaging devices like digital cameras or smart phones, motor car components like HID head lamps, projection displays, advanced safety systems and medical devices like endoscopes, eye inspection instruments, which are one of the strongest technologies of Japanese industries. Those precision optics recently contains a few aspherical lenses, which cannot be manufactured in conventional grinding and polishing method. Those aspherical optics are mostly manufactured by plastic injection molding or glass press mold using precision dies. Especially glass materials have strong advantage over plastics in terms of optical performance. To make an aspherical glass lens, glass press mold (GM) process is necessary, which use high precision dies made of tungsten carbide to mold glass preforms at temperature of 300 to 1000 degC. Since this molding process is conducted inside the heavy metal die at very high temperature, no attempt has been successful to investigate the process in real-time, whereas optimization of glass press mold condition is done by a number of trial-and-error.

Another issue in aspherical lens production is that there remains some inhomogeneity inside molded lenses, which is not easy to measure. A trial has been made to measure the optical path difference where molded lens is dipped in a high-refractive index liquid, but the stability

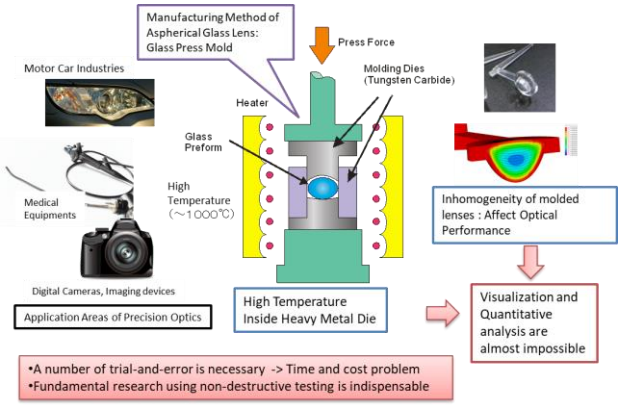

Fig. 1 Background of this Research

is not satisfactory. The final verification of such molded optics is conducted by assembly of all the prototype components, which is quite time-consuming.

Neutron Radiography can be one solution to analyze those issues, since the penetration depth of neutron beams in tungsten is rather good and most of glasses contain boron which is a good neutron absorber.

EXPERIMENTS: For FY2018, we have concentrated on developing a simulation code named V-Glace to understand the situation of glass press molding process. This code is based on V-Struct[1] system, which uses static explicit solver and hexahedral mesh system, which allow very large deformation without volume locking. The V-Glace code introduced a creep constitution to express glass molding process and thermal analysis. In addition, it has structure relaxation model to incorporate with glass relaxation mechanism.

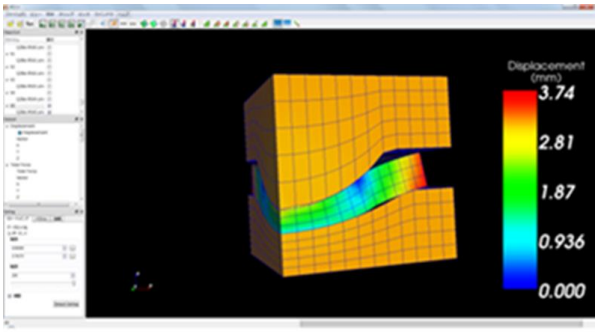

Fig.2 Screen of glass press mold simulation code.

Fig. 2 shows the screen of V-Glace software. It has pre-processor to generate hexahedral mesh from polynomial based aspherical lens profile and post processor to display stress, displacement with stress relaxation.

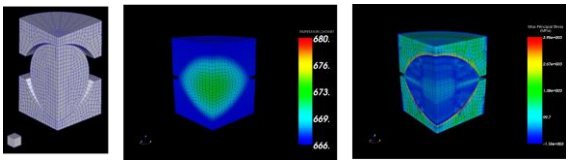

Fig.3 Glass molding simulation of ball-lens.

Fig.3 shows a simulation result of glass ball lens. Press molding process and stress relaxation (right) can be simulated[2].

RESULTS: Unfortunately, we were not able to perform neutron radiography for this year since preparation for molding process was not sufficient. We will try to do neutron radiography of glass molding process in the near future.

REFERENCES:

[1] Sun *et al.*, JSME Transactions A, **77** (773)(2011).
[2] Yamagata *et al.* JSPE Annual autumn meeting (2018).

PR2-8 Observation of Water Movement in Reciprocal Grafts of Tomato and Eggplant

U. Matsushima, R. Kobayashi, D. Ito[1], Y. Saito[1] and H. Shono

Faculty of Agriculture, Iwate University
[1] *Institute for Integrated Radiation and Nuclear Science, Kyoto University*

INTRODUCTION: Fruit sugar content of tomato plants grafted onto scarlet eggplants was higher than that of tomato plants grafted onto rootstocks of tomato [1]. These results suggest a way of obtaining high quality plant products, such as sweet tomato fruits, using this grafting technique. However, larger hydraulic resistance in *Solanum torvum* rootstocks than in tomato rootstock, has been shown to cause delayed graft-incompatibility [2]. We compared water movement at the graft union of tomato plants grafted onto tomato and eggplant, and eggplant plants grafted onto eggplant and tomato, to estimate the effect of graft-incompatibility.

MATERIALS and METHODS: Four types of grafted samples were prepared: tomato grafted onto eggplant rootstock (T/E) and tomato rootstock (T/T), and eggplant grafted onto tomato rootstock (E/T) and eggplant rootstock (E/E). Tomato (TO) and eggplant (EO) without grafts were prepared as control plants. Control samples were selected from seedlings that were sowed at the same time as seedlings for grafted plants. Fourteen days after grafting, we performed neutron imaging at the E2 hole of Kyoto University Research Reactor (KUR). Plant samples were fixed on a piece of thin aluminum board with aluminum tape. Thereafter, 10 mg of deuterium oxide (D_2O) was injected into the plant pot. Immediately after the injection, interval neutron imaging was initiated. Exposure and interval times were 300 s and 360 s, respectively.

RESULTS: The neutron cross section of D_2O is much lower than that of water. However, the chemical characteristics of D_2O are similar to those of water. Therefore, plants can uptake D_2O through the root system. The plant neutron image becomes bright as D_2O replaces water. The gray level of plant shoot images increased according to time after injection of D_2O. Figure 1 shows the changing ratio of the gray level (CRGL) from that of the initial value in the plant shoot images. Exceeding a CRGL value of 1 indicates that the gray level in the neutron image is increased. In Fig. 1, shoot length represents the length from the shoot part nearest to the root system, to the first true leaf. The CRGL of all samples was highest at the part near their root systems. The CRGL then decreased towards the upper part of the shoots. This indicates that water in the shoot vessel has been replaced by D_2O from the lower to upper part. Comparing the types of rootstock, the increase in CRGL was faster in the eggplant group than in the tomato group. In particular, the CRGL of T/E was the not only the highest among all the samples but also the fastest to pass over the value of 1.1. The dry weight of the T/E shoot was 79 mg/plant, which was the smallest of all shoots with an eggplant rootstock (EO had a dry weight of 113 mg/plant and E/E, 107 mg/plant). This fast D_2O uptake by T/E could not be explained according to shoot size. These results suggest that scion with eggplant rootstocks (T/E), require more water than other scion with eggplant rootstocks, EO and E/E.

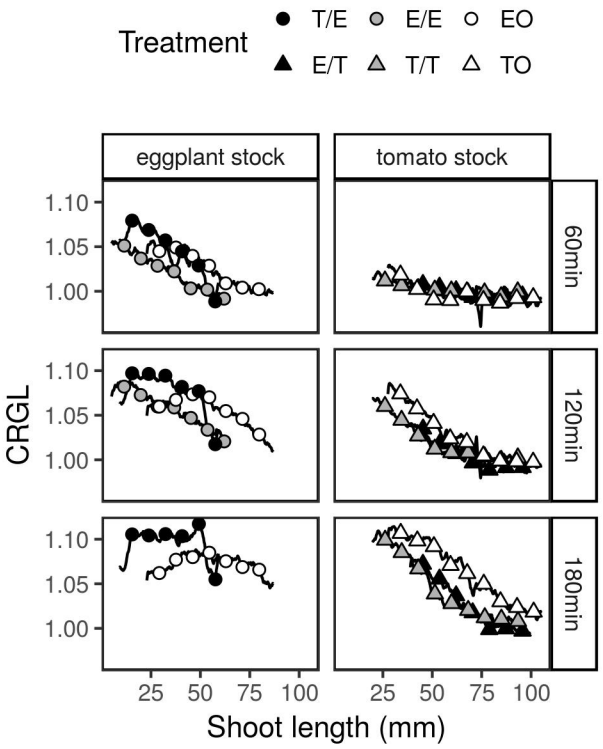

Fig. 1. Profiles of transmittance along plant shoots based on initial gray level. The transmittance is measured as the changing ratio of gray level (CRGL). The left-hand column of the graph shows plants with eggplant rootstock and the right-hand column shows plants with tomato rootstock. The rows of the graph indicate the time elapsed after applying D_2O.

REFERENCES:

[1] M. Oda *et al.*, J. Japan. Soc. Hort. Sci., **65(3)** (1996) 531-536.
[2] M. Oda *et al.*, J. Japan. Soc. Hort. Sci., **74(6)** (2005) 458-463.

PR2-9 Analysis of dehydration in high-strength concrete under high temperature using by neutron radiography

M. Kanematsu[1], Y. Nishio[1], A. Miyabe[1], K. Ueno[1], T. Koyama[1], D. Ito[2], Y. Saito[2], T. Noguchi [3], M. Tamura[3]

[1]*Department of Architecture, Tokyo University of Science*
[2] *The Institute for Integrated radiation and nuclear science joint-use research, Kyoto University*
[3] *Department of Architecture, The University of Tokyo*

INTRODUCTION: Concrete is commonly known as a material excellent in fire resistance, if ensure a constant cover depth, reinforced concrete (RC) structure is recognized as fire-proof structure in Japan's Building Standard Law. However, chemical and mechanical property of concrete is changed due to influence of high temperature, and damage of concrete suffered from heat is remaining after cooled down. Moreover, when RC structure is subjected to high temperature, surface layer of concrete could be peeled explosively. This phenomena is known as so-called "spalling". JCI reported the evaluation methods for spalling of high-strength concrete [1], such as ring test [2]. On the other hand, some researchers have been attempting to evaluate concrete as composite material composed of aggregate and cement paste matrix, which is representative volume element of meso scale [3].

Therefore, in this study, the authors applied neutron radiography (NR), an imaging technique by using neutron beam, to high-strength concrete under high temperature, and tried to measure water content with high spatial resolution. Furthermore, it was also tried to reveal dehydration of high-strength concrete under high temperature experimentally from the viewpoint of meso scale.

EXPERIMENTS: Mix proportion of concrete was prepared with W / B of 18%. For coarse inclusion, two types were used. One was graywacke from Ome for greywacke concrete, and the other was limestone from Sano for limestone concrete. Specimens were casted in mold of 100 × 100 × 400 mm, demolded after 24 hours and then cured in water until age of 28 days. After that, they were cut into sliced plates with a thickness of 20 mm and holes were produced in the specimens to install thermocouples. Until an experiment initiation, specimens were stored under 20°C RH 60% environment.

Thermocouples were installed in the holes drilled at the position of 10, 20, 40, 60, and 80 mm from the heating surface, respectively. Propane gas burner, controlled by flow meter, was used to raise the surface temperature. The surface temperature became constant in seconds after start of heating and was about 1000 °C.

NR was performed at Thermal Neutron Radiography Facility (TNRF) in the B-4 port by using neutron beams at the time of output 1MW steady-state operation. To minimize influence of scattered neutron

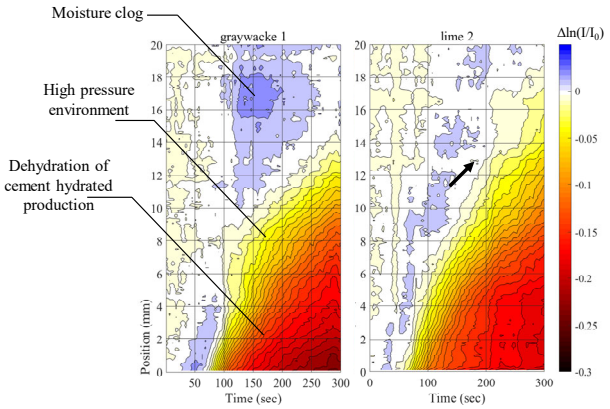

Fig.1 Legend and distribute of amount of substance per matrix unit

beams, distance between specimen and converter was set at 100 mm. Further, the angle of view of CCD camera was 100 × 100 mm, and the spatial resolution in this study was about 0.1 mm / pixel.

RESULTS: **Fig.1** shows contour plots which represent progressing and distribution of amount of substance per unit matrix. Dewater proceeding is indicated at black portion and increasing of water content is indicated at blue portion. With the specimen made of graywacke, **Fig.1** shows that regions of increased water content (moisture clog) are confirmed. Compared with the specimen made of limestone, moisture clog is larger. Therefore, it is considered that specimen made of limestone dissipate moisture easier than specimen made of graywacke from the weight reduction by heated. In addition, using the values obtained from relationship between temperature and decreased amount of substance per unit matrix, color map of contour plots was adjusted to indicate to evaporation of water in high pressure environment at yellow portion and to indicate to cement hydrate dehydrating at red portion. **Fig.1** shows that existence region of the high pressure environment had been moved to deep in specimen with the passage of time. Moreover, the existence region of the high pressure environment has been formed below the moisture clog.

REFERENCES:

[1] JCI, (2017). "Committee Reports:JCI-TC-154A Physical and Mechanical Properties of Concrete at High Temperature, Japan concrete Institut"

[2] M. Ozawa etc., (2014) "Numerical analysis of spalling of HSC restrained with steel rings at high temperatures, Proc. of Annu. Conv. of JCI, vol.36, No.1

[3] Jie Zhao, Klass van Breugel, (2014)." A meso-level investigation into the explosive spalling mechanism of high-performance concrete under fire exposure.", Cement and Concrete Research, vol.65, pp.64-75

PR2-10 Effect of gravity on coolant distribution in flat laminate vapor chamber

K. Mizuta, Y. Saito [1] and D. Ito [1]

Faculty of Engineering, Kagoshima University
[1] KURNS, Kyoto University

INTRODUCTION: Recently, rapid increase in heat dissipation from electric devices leads to various reliability problems and low working efficiency, then effective heat exhausting techniques are desired than ever. The author have developed flat laminate vapor chamber called FGHP (Fine Grid Heat Pipe), which consists of upper and bottom plates, and of some middle plates. All the plates are made of copper, and the coolant used was water. As for thermal performance, FGHP had the lowest thermal resistance among various vapor chambers when the effect of heat receiving area is concerned [1], and the lateral thermal conductivity exceeded 10,000 W m^{-1} K^{-1} when the temperature of heat receiving area exceeded about 360 K [2]. Moreover, the liquid thickness in the wick area scarcely changed with heat input even when the surface of FGHP was set parallel to the gravity direction [3]. In our previous study [3], however, the heat input was below about 15 W, which were smaller than that in the practical use.

In this study, we investigated the gravitational effects on the coolant distribution in the FGHP by using neutron radiography at the Kyoto University Research Reactor (KUR) when the heat input is larger than that in our previous work [3].

EXPERIMENTS: Experiment was conducted at the E-2 port of the KUR, where the thermal neutron flux at the sample position was about 3×10^5 cm^2s at 5 MW operation. The size of the test sample of FGHP heat spreader was 65 mm square and 2 mm thick. The test sample was set vertically, which means that its bottom and top plate was placed parallel to the gravitational direction. A ceramic heater of $25\times25\times1.75$ mm^3 was attached to the central part of the bottom plate as a heat source, and the top plate was cooled by plate fin type heat sink under forced convection conditions. K-type thermocouples were utilized to measure both the surface temperature of the heat spreader and the atmospheric temperature to estimate the thermal resistance of the FGHP. A CCD camera (BU-53LN, BITRAN Co. Ltd.) was utilized, which has 4008×2672 pixels and ^{6}LiFZnS (50 μm thickness) was used as a scintillator screen. The spatial resolution was 9.0 μm/pixel at the present system setup, however, the effective spatial resolution was about 50 μm/pixel due to the scintillator screen characteristics. Neutron imaging of the sample was performed at the 1 MW operation mode of the KUR and the exposure time was 300 s. Neutron images of the sample were utilized to calculate liquid thickness in the FGHP. The effect of gravity on the coolant distribution was evaluated by the calculated liquid thickness in the wick area at different positions as follows:

1. Vertical position 1 (Top),
2. Vertical position 2 (Bottom),
3. Horizontal position 1 (Left),
4. Horizontal position 2 (Right).

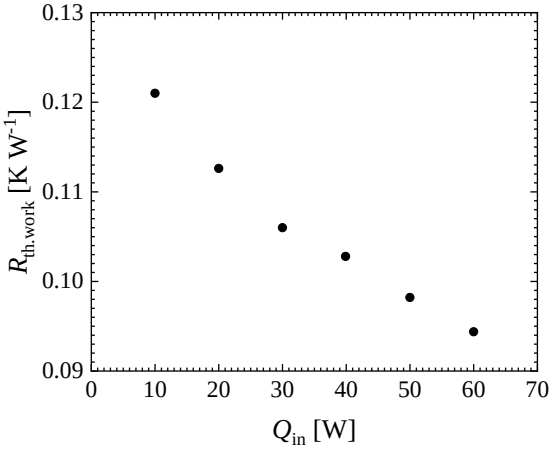

Fig. 1 Variation of the thermal resistance of the test sample with heat input.

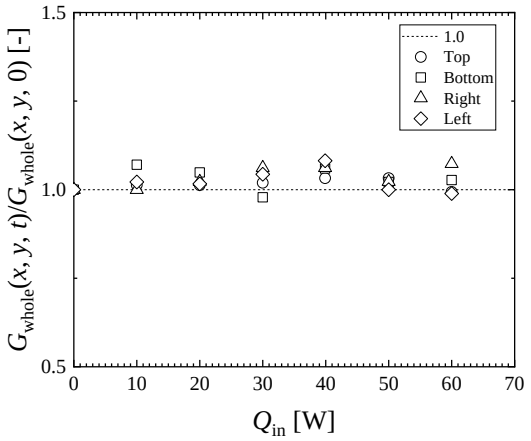

Fig. 2 Variation of the averaged gray level with heat input.

Interrogation window size was 0.4×1.5 mm^2 at each position.

RESULTS: Figure 1 shows the variation of thermal resistance of the test sample with heat input. As shown in Fig. 1, thermal resistance of the test sample decreases with increasing heat input as reported in the previous work [1], which shows that this test sample worked properly under the current experimental conditions. Figure 2 shows the variation of the averaged gray level in the respective interrogation area with the heat input. As shown in Fig. 2, the values of averaged gray level are nearly constant regardless of heat input, which suggests that the thickness of liquid film in the wick area was scarcely affected by the heat input under the current experimental conditions.

REFERENCES:

[1] K. Mizuta *et al.*, App. Therm. Eng., **104** (2016) 461-582.
[2] K. Mizuta *et al.*, App. Therm. Eng., **146** (2019) 843-853.
[3] K. Mizuta *et al.*, Phys. Proc., **69** (2015) 556-563.

PR2-11 Study on the Visualization of Organic Matter between Metals in oder to Contribute to the Advancement of the Industrial Products

K. Hirota, H. M. Shimizu[1], M. Kitaguchi[1], Y. Tsuchikawa[1], S. Imajo[1], S. Awano[1], N. Yamamoto[1], A. Uritani[2], K. Watanabe[2], S. Yoshihashi[2], A. Yamazaki[2] and Y. Saitoh[3]

RCNP, Osaka University
[1]Graduate School of Science, Nagoya University
[2]Graduate School of Engineering, Nagoya University
[3]Institute for Integrated Radiation and Nuclear Science, Kyoto University

INTRODUCTION: Mechanical and industrial products such as automobiles and aircraft are progressing with higher performance and higher accuracy in Japan. One of the demands at the development site of these state-of-the-art products is visualization of the state of organic materials (oil film, grease, electrolyte, etc.) existing between metals, which can not be seen directly by our eyes. In this research, we will explore the possibility of observing the dynamic state of the organic materials (shape, properties, thickness distribution) and its dynamic change mainly between automobile parts as an example.

At present Nagoya University is constructing an accelerator-driven small neutron source (NUANS) and neutron radiography ports [1,2]. We are planning an in-site measurement of fuel cell during the power generation. And we are also proceeding with the quantitative evaluation of the CCD output image. This year, we produced a neutron camera for radiography to be used at NUANS, so we evaluated its performance in KUR E2 port.

EXPERIMENTS: In the fuel cell development, the elimination of water from the electrode during the power generation is very important issue. It was evaluated whether water droplets generated during fuel cell power generation could be identified or not, using fuel cell electrodes by neutron radiography measurement. Since the fuel cell uses a combustible gas, it is impossible at KUR to make measurement while actually generating electricity. So we put water directly into the fuel cell electrodes, and measured the transmission image at E2 port, not using the combustible gas. At the result, we cans see the clear image with 60s neutron irradiation.

In addition, a space of about 1 mm^3 was made on an aluminum plate, water droplets were placed, and measurements were made for a short time, to evaluate how much visual time would be visible in what measurement time. At the result, we can see the water drop is clearly seen with the 1s irradiation time. Next we tried to move the water position quickly, and we also could see the water position.

CFRP(carbon fiber reinforced plastic) is considered to be a effective material for near-future industrial use as a lightweight and durable material. Although it is a strong CFRP, fatigue failure can occur, so when we use it to aircraft we have to evaluate and identify the precursor crack. CFRP is usually covered with aluminum on the surface, X-ray transmission measurement is difficult to see. Neutron transmission imaging is good candidate to check the cracks of CFRP.

Since the CFRP contain a large amount of hydrogen, it is also difficult to measure even in the neutron radiography. And because it has a layered structure, it is desirable to identify the position of the crack in the depth direction by performing CT measurement. In this measurement, we try to get the transmission image and CT measurement of a joined body of CFRP and aluminum alloy, which are 3cm width and 5mm thickness, respectively. In the first trial, we can get the 3D image of CFRP and aluminum joint material, and the crack image is not so clear. We will get the better image to scrutinize the measurement conditions.

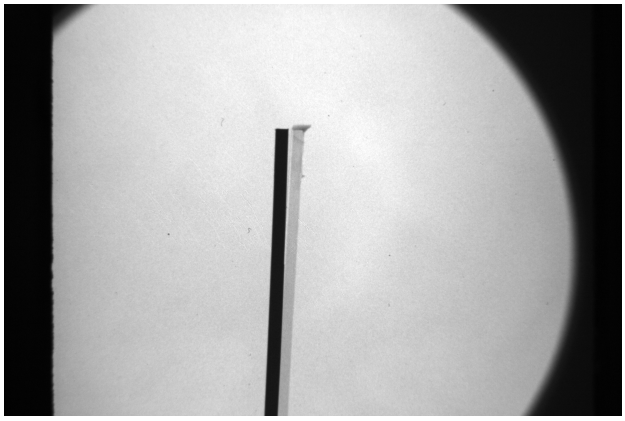

Fig. 1. Measurement of the peeling of CFRP and aluminum alloy.

REFERENCES:

[1] K. Hirota, PoS., (KMI2017) 025.
[2] I. Ito, PoS., (KMI2017) 068.

PR2-12 Development of canalicular-structure-based neutron optical devices

T. Sakai[1], H. Iikura[1], D. Ito[2] and Y. Saito[1, 2]

[1]*Materials Sciences Research Center, Japan Atomic Energy Agency*

[2]*Institute for Integrated Radiation and Nuclear Science, Kyoto University*

INTRODUCTION: In this work, we are developing two neutron devices, namely micro-structured fluorescent plates and Soller slits. The former device consists of capillary plates and fine phosphor grains [1, 2]. The capillary plates are commercially available glass plates on which tiny capillaries are arrayed in two-dimensions periodically [3]. The latter is based on commercial canalicular-structured ceramic devices. Herein, we introduce the development of the Soller slits for neutron optical device.

EXPERIMENTS: The ceramic device is named HONEYCERAM ™ and manufactured by NGK INSULATORS, LTD. [4]. The original ceramic and sliced ones are shown in Fig. 1 (a). The magnified image of the entrance of the ceramic canals is indicated in Fig. 1 (b). The canal size is approximately 0.7 mm x 0.7 mm, and the wall is mere 0.05 mm thick. The outside diameter is 106 mm, and L/D ratios are 11, 30, 163 for 8 mm-length, 21 mm-length, 114 mm-length, respectively. The ceramics are impregnated with gadolinium acetate solution to add neutron absorption capacity. The first test of fabricated Soller slits was performed at KUR E-2. The photograph of the experimental setup and the neutron radiograph were shown in Fig. 2.

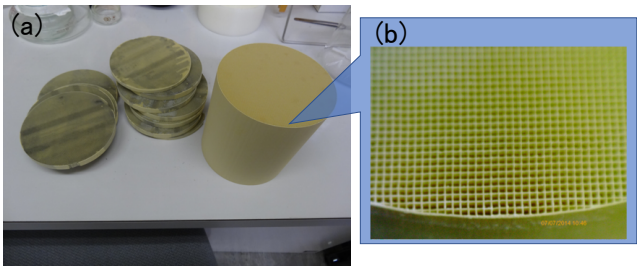

Fig. 1 Photographs of HONEYCERAM ™ and sliced ones (a), and magnified image (b).

RESULTS: The radiograph in Fig. 2 (b) indicated that the ceramic worked well as Soller slits. The neutron absorption in the wall is fairly uniform, though some canals are clogged with shavings. The dependence of neutron transmittance on the slits length is not evaluated yet.

The fabricated Soller slits are expected to be useful to improve the neutron beam parallelism, namely L/D ratio. Impregnation with gadolinium acetate solution is effective to add neutron absorption capacity to the ceramic wall. The fabrication method is simple, and the materials are relatively cheap (~10,000 yen).

The next step of the work is characterization the slits performance and application to the imaging experiments.

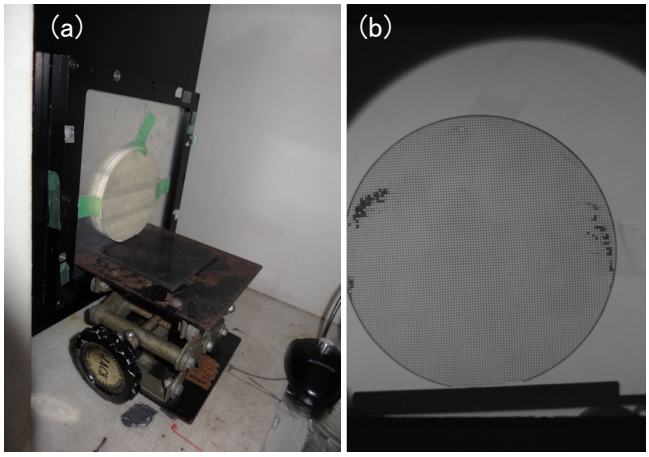

Fig. 2 Photograph of experimental setup at KUR E-2 (a) and the neutron radiograph of the fabricated Soller slits (b), respectively.

REFERENCES:

[1] T. Sakai *et al.*, JPS Conf. Proc. 11, 020005 (2016) .

[2] T. Sakai *et al.,* KURRI PROGRESS REPORT 2017, 29P7-14 (2018) .

[3] HAMAMATSU PHOTONICS K. K. website: <http://www.hamamatsu.com/jp/en/product/category/3200/3032/index.html>

[4] NGK INSULATORS, LTD. website: <https://www.ngk-insulators.com/en/product/automobile/>